RSC Advances

ROYAL SOCIETY OF CHEMISTRY

www.rsc.org/advances

Synthesis and optoelectronic characteristics of 20-nm-diameter silver nanowires for highly transparent electrode films

*Eun-Jong Lee[1], Yong-Hoe Kim[1], Do Kyung Hwang[2], Won Kook Choi[2], and Jin-Yeol Kim[*1]*

[1]School of Advanced Materials Engineering, Kookmin University, Seoul 136-702, Korea

[2]Interface Control Research Center, Future Convergence Research Division, Korea Institute of Science and Technology (KIST), Seoul, 136-791, Korea

ABSTRACT

We demonstrate the polyol synthesis of ultrathin Ag nanowires with diameters of 20-nm and an aspect ratio as high as ~1000 at the high-pressure condition. With the pressure increase, increases density and enhances solubility, making the reactive solution rapidly reach super-saturation, and could increase the nucleation rate to effect near-instantaneous forming of Ag nuclei. Clearly, particle size is smaller at high pressure and increasing the pressure was promoted the formation of small-size Ag seed-particles and small diameter wires. As a result, the Ag nanostructures in this study initially formed as Ag seed particles with a diameter of 20 nm, and subsequently grew into well-defined Ag nanowires with a narrow diameter distribution, uniform, through the range of 16–22 nm, with a long dimension of up to 20-μm. Fabrication of random networks of synthesized 20-nm-diametered Ag nanowires leads to the fabrication of flexible transparent electrodes with excellent optoelectronic performance, with a sheet resistance of 30 Ω/sq, 94 % transmittance with a very low haze value of ≤1.0%, making them, suitable for electronic display applications.

KEYWORDS

20-nm Ag nanowire, high-pressure polyol process, transparent electrode, haze value, organic photovoltaic cell

1. Introduction

Transparent electrode films (TEFs) have recently attracted a great deal of attention in the various flexible optoelectronic devices, such as large-area touch screens, thin-film solar cells, and organic light emitting diodes (OLEDs). In currently, they are made from a sputtered film of indium tin oxide (ITO) due to its high optical properties (up to 90% transmittance and ~1% haze) at low sheet resistances of down to 60 Ω/sq.[1] However, the high conductivity ITO used in these TEFs, for flexible optoelectronic devices, is particularly costly due to the slow coating rates and high temperature/vacuum processing conditions involved with roll-film sputtering. This has motivated the research for solution-processable alternative to ITO that can be fabricated at high speeds, low costly processing conditions and give comparable performance. There are several solution-coatable alternative to ITO, including carbon nanotubes, graphene, conducting polymers (PEDOT:PSS), and silver nanowires (Ag NWs), but only commercially available Ag NWs have demonstrated optoelectronic performance that exceeds that of ITO. Thus, Ag NWs electrodes have been gaining interest as a promising alternative to ITO due to the ease of manufacture, large scale solution processability, highly conductivity with mechanical ductility.[2-13] Ag NW with well-defined small diameters with large aspect ratio are particularly focused, as they have good optical due to the less scattering light, and plasmonic properties, making them excellent candidates for transparent electrodes. However, in order to achieve the required optical and electrical characteristics, there is still a need to develop more effective processes for synthesizing Ag NWs with controllable shapes and sizes, in particular, a continuous range of lengths up to at least 20-μm and a diameter of 20-nm to make effective network junctions between the Ag NWs and high optical property.

Ag NWs are typically synthesized in solution, using the polyol method that was originally developed by Xia et al.,[14-17] to demonstrate their potential as a transparent electrode with satisfactory electrical and optical performance. These studies typically focus on controlling the size, shape, crystal structure, and optical/electrical properties of the Ag NWs. The electrical conductivity of these 2-D film structures consisting of Ag NW networks is reported to be approximately 0.8×10^5 S/cm, while the sheet resistance of a 2-D percolating Ag NW network exhibits a value of 30 Ω/sq; optical transmittance is approximately 90 %. This conductivity value almost matches with that of the conventional crystallized-ITO on the glass (~30 Ω/sq at 94% transparency: substrate base) in electrical performance; however, in optical performance, their transmittance is generally lower. In addition, the haze value of Ag NW films is known to be higher because of the wire geometry and the high light scattering characteristic of Ag. In fact, it is difficult to fabricate sufficiently transparent electrode films using a network of thick Ag NWs because a significant part of the light is scattered from the uneven nanowire surface. This high scattering can cause blurriness particularly if used in a display's transparent electrode, and currently, it is required that optical haze to level of ITO. Conventional ITO exhibit a haze of approximately 1~1.5 % with a sheet resistance of 30~50 Ω/sq at a transparency of up to 94% (substrate base) and have been used in display devices.[18, 19] However, Ag NW electrodes at 90% transmission can achieve still low sheet resistance of 20~60 Ω/sq because of the high conductivity of Ag, but their high haze value of up to 2% is a major disadvantage for the application of Ag NW electrodes in display devices. If the haze can be decreased to the level of ITO, in combination with the high conductivity, Ag NW electrodes can be opened new frontiers in terms of applications in devices. Optical haze is also an equally important yet unstudied parameter in the Ag NW transparent electrodes for solar cells, the haze refers to the degree of

incident light scattered forward towards the absorber layer, which enhances the path length of light of the OPV.[5] Hu *et al.* [5] provided the study of haze properties for Ag NWs, and investigated the haze factor of Ag NWs with relatively large and small diameters theoretically through their scattering behavior in OPV. With respect to the optical haze of the Ag NWs, Han *et al.*[18] reported that the haze of Ag NWs electrodes film with an average length of 13.5 μm in length and 62 nm in diameter showed at approximately 3% when the transmittance exceeded 95% with sheet resistance of 30 Ω/sq. Suganuma *et al*.[19] demonstrated that the haze can be reduced by increasing the length of Ag NWs. They reported a low haze value of 2.2 % with a sheet resistance of 49 Ω/sq and 94% transmittance from long Ag NWs of up to 200 μm. We also demonstrated the synthetic method with optoelectrical properties of Ag NWs with 30- and 45-nm-diameter using the polyvinylpyrrolidone-assisted polyol method in the presence of ionic liquids which served as soft template salts.[20] The 30-nm diametered Ag NWs showed the sheet resistance of 30 ohm/sq with transmittance of 93% and haze of approximately 2.0%. Thus, we could be obtained a good conductivity and transmittance values, but their haze value was slightly high. However, these haze value of up to 2% was an insufficient value compared to ITO for the application of Ag NW electrodes in display devices. In order to decrease the haze while maintaining the high conductivity, it is necessary to extend the length or decrease the diameter of the wires to make network junctions between the Ag NWs. In general, extending the length and decreasing the diameter of wires have been expected to be a promising strategy to achieve low haze with high conductivity and high transparency. Moreover, smaller diameter Ag NWs directly decreases the haze in the visible wavelength because of the decreasing scattering of light.[21] To achieve sufficiently transparent electrode films having a low haze value of less than 1.5 % (level of ITO) with 30 ohm/sq sheet resistance for applications, thin and long Ag NWs are required, up

to 20-μm in length with at least 20-nm diameter. In efforts to reduce haze, several synthesis methods have been used to create thinner and longer NWs with reduced junction resistance. We first reported in a previous letter the basic concepts of how Ag NW synthesis can be controlled to yield diameters in the range of 20–30 nm with lengths of approximately 15 μm, using an elevated pressure of 250 psi in a high-pressure polyol reaction.[22] At the time, the reaction mechanism was not fully explained and a demonstration of the reduction of optical haze in transparent electrodes was not carried out for applications to electronic devices.

In this work, to produce Ag NWs with better electrical and optical performance, we successfully synthesized ultrathin Ag NWs at large scale reactor of 2L, with diameters in the range of 16−22 nm and an aspect ratio as high as ~1000, using high-pressure polyol reaction under 1000 psi (69 bar) conditions. Fabrication of random networks of Ag NWs leads to flexible transparent electrodes with excellent optoelectronic performance, namely a sheet resistance of 30 Ω/sq at 94 % transmittance and a very low haze value of ≤1.0%, suitable for electronic display applications. This electrical performance matches the properties of crystallized-ITO films, and in optical performance, their haze value is almost the same as that of ITO films.

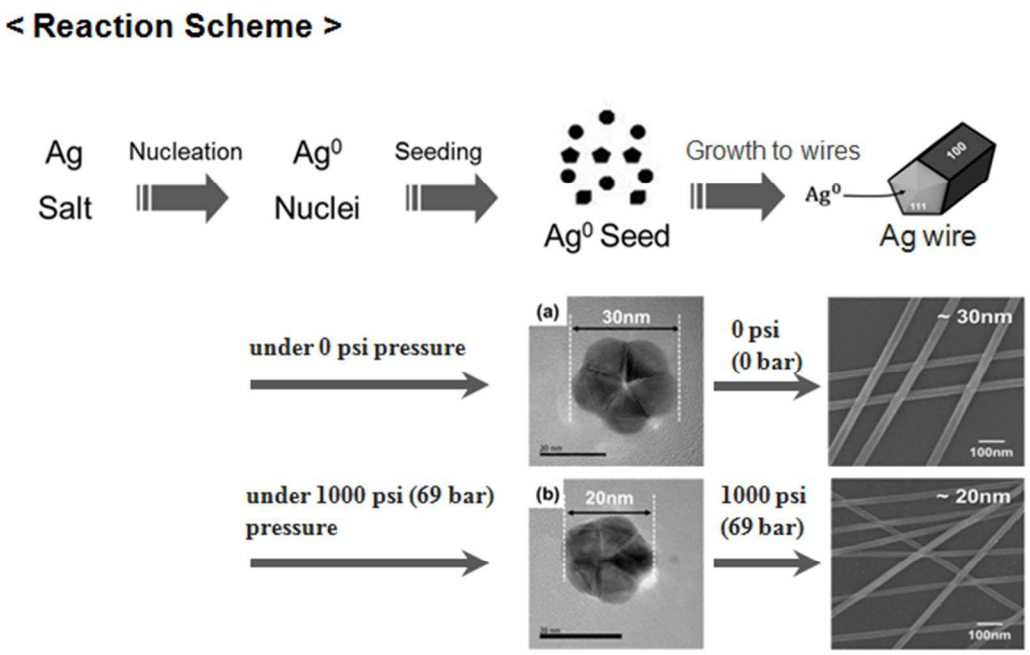

Figure 1

2. Experimental

All reagents and chemicals were purchased from commercial sources (Aldrich, Fluka, Acros) and used without further purification. Ultrathin Ag NWs were synthesized through a high-pressure polyol method by chemical reduction of $AgNO_3$ (Aldrich) with PVP (average molecular weight, M_w=1,300,000, Aldrich) as a capping agent, and in the presence of a NaCl solution or combined salt solution (NaCl and KBr). The 20-nm diameter Ag NWs has been synthesized by the following method. First, 3.78 g of PVP was dissolved concurrently in 400 mL of ethylene glycol (EG) under vigorous stirring. Then, 128 mg of NaCl and 130 mg of KBr were added in PVP solution, and the mixed solution was transferred to an 2L size autoclave reactor using a syringe pump and stirred for 1 h at 200 rpm under 1000 psi (69 bar) pressure and 160 ºC temperature. In the second step, 3.24 g of $AgNO_3$ solution (0.06 mol in EG) was quickly added

into the autoclave reactor using a syringe pump, and the reaction was maintained for a further 1 h under 1000 psi (69 bar) of N_2 and 160 ºC. The reactor was then cooled to room temperature, and the yield of the obtained wires before purification is from 85 to 90% (determined by the silver ion contents analysis through ICP). After synthesis, the products were purified by acetone and centrifuged at 1000 rpm for 90 min to remove the solvent (EG), PVP, and other impurities. After the final centrifugation, the precipitates were re-dispersed in H_2O. And, the 30-nm diameter Ag NWs was synthesized in the same process as that of 20-nm diameter Ag NWs under atmospheric pressure condition. The Ag NWs with 40-nm diameter was prepared in NaCl alone solution instead of combined salt solution and atmospheric pressure condition.

The Ag NWs, with approximately 20-nm, 30-nm, 40-nm diameters, were dispersed in DI water for an optimized density of 0.5 mg/mL and directly deposited on an O_2 plasma-treated polyester (PET) substrate film by a commercially available wet coating method through Mayer bar coating technique to fabricate the transparent electrode film. The density of Ag NW deposition was controlled by the volume of coated solution, determined by the speed of the spin coater or by the mesh size (# 3, 5, 9, and 16) of the Mayer bar. The mesh size of the Mayer bar was determined depending on the thickness of the coating film layer that requires.

The highly conductive Ag NWs electrode films are fabricated without any post-treatment.

The morphology and molecular structures of the dispersed Ag-NWs were observed by field emission scanning electron microscopy (FE-SEM, JEOL-JSM5410) and transmission electron microscopy (TEM, JEOL-JEM2100F). The optical and surface Plasmon resonance (SPR) spectra were measured by ultraviolet spectroscopy (UV/vis, SHIMAZU-UV3150) and Haze mater (NDH 7000). The electrical properties of the Ag NW films were measured using a standard four-point probe technique (Laresta GP, MCP-T60).

Flexible OPVs were fabricated on Ag NW/PET substrates. For the conventional device arearchitecture, PEDOT:PSS (Clevios^{TM} P VP AI 4083) was spin coated at 100 nm-thick onto the electrode layer and annealed at 130 °C for 30 min. poly(3-hexylthiophene) (P3HT) 18 mg (Rieke metals, Inc.) and [6,6]-phenyl-C61-butyric acid methyl ester ($PC_{60}BM$) 10.8 mg were dissolved in 1 ml of chlorobenzene; the solution was spin coated at 2500 rpm for 40 s and annealed at 150 ^{o}C for 13 min in a glove box. The thickness of the active layer was approximately 100 nm. Finally, the LiF (0.6 nm) and Al (100 nm) electron-collecting and top electrodes were prepared by thermal evaporation in atmosphere. For the reference devices, ITO electrodes on glass substrates (JMC Glass, 30 Ω/sq at 94% transparency) were used; all fabrication processes were identical. Solar cell properties were measured with a solar simulator (ORIEL) having a 150 W light source. The standard light source was calibrated by a standard Si photodiode to realize the AM 1.5 condition and an intensity of 100 mW/cm^2.

3. Results and Discussion

The initial polyol synthesis was introduced by Fiévet et al.[23] as a simple way to obtain metal particles by reduction in liquid polyol. Recently, Xia and co-workers,[14-17] based on the PVP-assisted polyol method, demonstrated a salt-mediated polyol process using NaCl, $CuCl_2$, $PtCl_2$, or CuCl, to prepare Ag NWs of 30–50 nm diameter in large quantities. The synthesis takes place in two steps as shown in Figure 1: an initial seeding step and a growth step, obtaining octahedral-structured metal seeds and pentagonal-structured Ag wire, respectively. The first step involves the formation of Ag seed particles by nucleation from $AgNO_3$ in ethylene glycol solvent. These Ag particles act as seeds, which grow into wires in the presence of $AgNO_3$ and poly(vinylpyrrolidone) (PVP). PVP is a surface-capping reagent, which kinetically controls the

growth rate of the metal surfaces and subsequently induces 1-D growth, leading to formation of NWs. As a capping agent, it prevents aggregation of nanostructures, controlling their size and shape; it also acts as an inducing agent to lead 1-D crystal growth along the [110] direction, due to selective absorption of PVP on different crystal faces. Control of seed particle structure during synthesis is therefore very important in determining the shape of Ag NWs formed. Generally, this polyol process is done at atmospheric pressure. In this work, as in previous studies, we synthesized Ag NWs through $AgNO_3$ reduction in ethylene glycol/PVP in the presence of mixed KBr and NaCl salts, under atmospheric pressure.

The reaction scheme shown in Fig. 1-(a), for atmospheric pressure forms, Ag seed crystals of approximately 30-nm size with a multi-twin structure through reduction of $AgNO_3$ as the first step; these Ag seed particles are then grown to wires with diameters of about 30-nm. In the present study, under a the N_2 pressure of 1000 psi (69 bar) (Fig. 1-(b)), the Ag seed particles and Ag NWs were approximately 20-nm in size and about 20-nm in diameter, respectively. In addition, size and shape of the Ag nanostructures was controlled by the presence of the mixed salts (KBr and NaCl) with PVP. The ratios of KBr and NaCl to the $AgNO_3$ precursor, as well as the pressure, are parameters in controlling the growth of Ag nuclei and seed particles during synthesis of Ag NWs in the ethylene glycol solvent. Thus, NaCl and KBr salts to the $AgNO_3$ precursor act as the groups in controlling the growth of Ag nuclei, and the nucleation rate of Ag ion has been also known to be in close relationship with the product size. In the presence of NaCl, the AgCl particles, which serve as twined nuclei for growing into twinned seed particles, could be easily formed. Here, the combination of Ag^+ and Cl^- reduced the concentration of silver ion, and thus effectively increased the percentage of twinned seed particles. However, for NaCl salt, through it was size change of the products when increasing the concentration of the nucleants to

mole ratios of 0.0065 or increasing it to 0.167, the diameter of Ag NW products never dropped below 40 nm, as shown in Fig. 2 (a). KBr salt can be also combined Ag ion to from AgBr particles, the nucleation rate was enormous and the size of the generated nucleus has been reported to be smaller than NaCl. Thus, these twinned seed particles formed from KBr solution are formed be so small that they transferred into other shaped particles via fluctuation before growing axially into wires. However, we could demonstration that the NaCl effectively formed the twinned seed particles and the concentration of excess KBr can inhibit the growth of the diameter direction in wire growing step. Thus, Br ion acts to inhibit to growth in the thickness during wire growth and it effect is increased efficiently by applied pressure. Accordingly, in this experiment, KBr and NaCl were utilized as a co-nucleant to increase the nucleation rate to an appropriate level, then it is possible to decrease the size of Ag NW in the final product.

Figure 2 compares a conventional atmospheric pressure process at 160°C to other a pressure conditions, for mole ratios of $NaCl/AgNO_3$= 0.0065 (low concentration) and 0.167 (high concentration), with PVP (M_w=1,300,000) as a capping agent. According to previous report[21], the suitable amount of NaCl is required in forming the Ag NWs in a conventional polyol process. It is because increasing the probability of forming pentagonal twinned seeds which can grow to wire shape. Here, Mole ratio of $NaCl/AgNO_3$= 0.0065 is a suitable concentration for the growth of Ag NWs. The shape of wire is also affected by the concentration of NaCl. In the case of $NaCl/AgNO_3$= 0.167 or higher molar ratio, there showed a difference in the amount of forming AgCl. As a results, it caused to be generated a lot of by-products such as particles. As shown in Figure 2-(a), for the reaction without KBr present, Ag NWs with 50-nm and 40-nm diameter are obtained for low and high concentrations of NaCl, respectively, but their dimensions are not changed by pressure. However, when KBr is used with NaCl in the ratio of 1:2, the diameter of

grown Ag NWs decreases with increased pressure. As a result, at a pressure of 1000 psi (69 bar), Ag NWs with diameters of approximately 20-nm were obtained from this process, with pressure initially controlling the size of the Ag seed crystal. Figure 2-(b) shows the Ag NW diameter as a function of KBr concentrations in the range 0−2.0mM, for low and high concentration of NaCl and at both 0 and 1000 psi (69 bar). The diameter is significantly decreased by increased KBr concentrations, especially at the higher pressure. From these indication, KBr acts to inhibit to growth in the radial direction during wire growth, and at the same time, it effect is increased efficiently by applied pressure. However, halide ions play an important role in the polyol reactions of Ag NWs. In particular, Cl ions effectively formed the pentagonal twinned seed and Br ions was inhibits the growth of the diameter direction in wire growing step. Here, Mole ratio of $NaCl/AgNO_3$= 0.0065 is a suitable concentration for the growth of Ag NWs. The shape of wire is also affected by the concentration of NaCl. In the case of $NaCl/AgNO_3$= 0.167 or higher molar ratio, there showed a difference in the amount of forming AgCl. As a results, it caused to be generated a lot of by-products such as particles. The synthesis of 20-nm diameter Ag NWs was carried out divided into two steps. In first step, PVP and NaCl/KBr were dissolved in EG solution under vigorous stirring for 1 h at 120 ºC, and in second step, $AgNO_3$ solution was quickly added into the autoclave reactor and the reaction was maintained for a further 1 h at 160 ºC. In particular, the reaction time in the second step is closely related to the growth rate of the wire, and it was possible to obtain the highest wire products when the reaction time was 1 h. On the other hand, if the reaction time is longer than, the diameter growth of the wire is enlarged and thickened as the by-product produced in the form of particles.

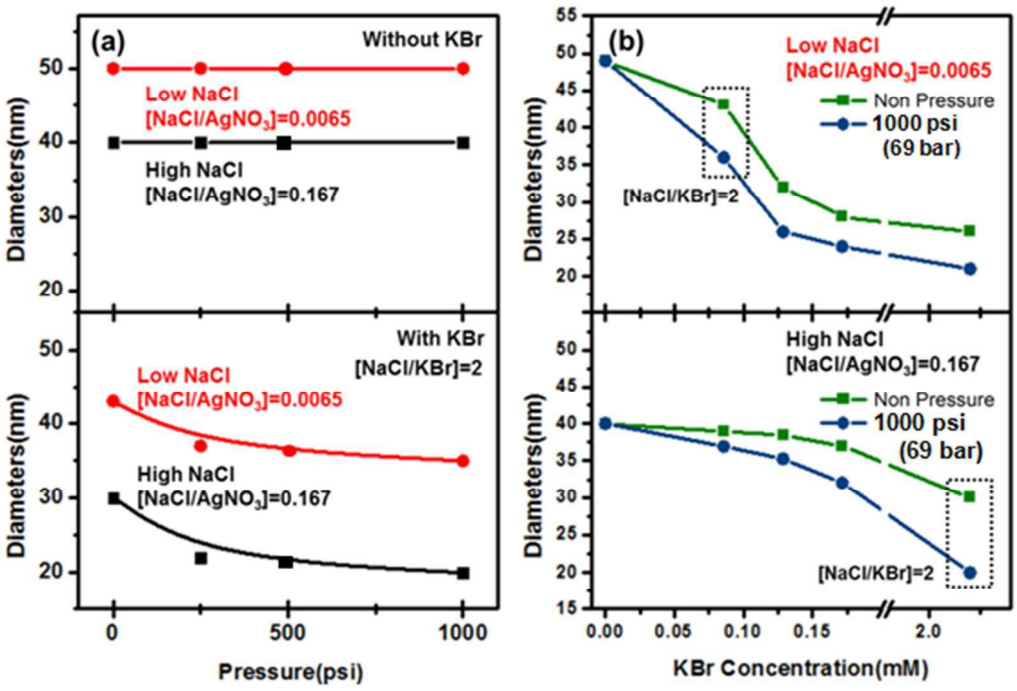

Figure 2

The Ag NWs synthesized by the high pressure polyol reaction are clearly smaller and have a more uniform dispersion than those made by the conventional atmospheric pressure process. The effect of pressure on the reaction solution is to promote synthesis of seed particles and wires and enhance the reaction rate. It can reduce solvent viscosity and increase the contact frequency of silver ions (Ag^{+}) and electrons (e^{-}), and thereby be as important to process rates as temperature and chemical composition. As a result, smaller sized particles and a faster nucleation rate are produced. The role of the pressure factor on the growth mechanism of Ag NWs has been described, Liao and co-workers[25] using classical nucleation theory and is expressed in Eq. (a).

$$\text{(a)}\quad \Delta G^{*} = \frac{16\pi\gamma^{3}}{3\Delta G_{v}{}^{2}} \xrightarrow{\text{Partial differential}} \left(\frac{\partial \Delta G^{*}}{\partial P}\right)_{T} = \left(\frac{3\Delta G^{*}}{\gamma}\right)\left(\frac{\partial \gamma}{\partial P}\right)_{T} - \left(\frac{2\Delta G^{*}}{\Delta G_{v}}\right)\left(\frac{\partial \Delta G_{v}}{\partial P}\right)_{T}$$

Equation (a) invokes the variable energy barrier (ΔG^*) to include pressure effects. Here, ΔG^* expresses the result of nucleation associated with a reduction in concentration of Ag ions (Ag^+). The factor γ is the interfacial energy, and ΔG_v is the difference in Gibbs' free energy per unit volume. The variation of ΔG_v with pressure is then expressed by a differential at constant temperature. Compared to ΔG_v, pressure variation of interfacial energy is small and can be ignored. As pressure increases, the energy barrier of nucleation lowers, decreases, accelerating nucleation. According to phase transition theory, the ratio of growth rate to nucleation rate determines crystalline grain size, or equivalently, particle size will be smaller at increased nucleation rates. Therefore, particle size decreases with increasing pressure.

However, in this experimental result, we observed that the growth process produced smaller and more dispersed particles with high-pressure polyol. Furthermore, increasing the pressure increases density and enhances solubility, making the reactive solution rapidly reach super-saturation, and can increase the nucleation rate to effect near-instantaneous forming of Ag nuclei. Clearly, particle size is smaller at high pressure and increasing the pressure may promote the formation of small-size Ag seed-particles and small diameter wires. As a result, the Ag nanostructures in this study initially formed as Ag seed particles with a diameter of 20 nm, and subsequently grew into well-defined Ag NWs with a narrow diameter distribution, uniform, through the range of 16–22 nm, with a long dimension of up to 20-μm (aspect ratio is approximately 1000), as shown in Figure 3. Figure 3-(I) and (II) display SEM and TEM images of the thin Ag NWs synthesized at a pressure of 1000 psi (69 bar). The TEM images indicate that the diameter of each individual nanowire is uniform along its length, with a narrow size distribution in the range of 19–22 nm. From the structural analysis of the side and the tip area of Ag NWs through the high-resolution TEM, along with the selected area electron diffraction

(SAED) image, we could be also obtained further insight into the structure of the Ag NWs in which the NWs were determined to grow along the [110] direction.

The X-ray diffraction (XRD) pattern for the sample prepared here indicates that the crystal structure of these nanowires is face-centered cubic (fcc). Figure 3-(III) displays the XRD patterns, and it is seen that all diffraction peaks can be indexed as the fcc phase of Ag. It is worth noting that the intensity ratios of the [111] and [200] reflections exhibit relatively high values, indicating a preferred [111] orientation of the Ag NWs. The longitudinal axis was oriented along the [110] direction. Previous studies have indicated a low threshold for twinning parallel to the [111] faces of silver, as inferred from grown bi-crystals that were twinned along the [111] plane.[26]

Surface Plasmon resonance (SPR) was also used to identify optical characteristics of the Ag nanostructures produced, as shown in Figure 3-(IV). It is well documented that Ag nanostructures exhibit a wide range of optical phenomena specifically related to SPR, such as absorption and scattering of light, with characteristics that depend on the geometry and size of the metal particles.[27, 28] An SPR spectrum can be fundamentally used to determine the size and shape of Ag NWs by examining the SPR bands that appear at different frequencies. According to previous reports,[28, 29] the characteristic main SPR peaks for Ag NWs with diameter of 30–60 nm appear between 372 and 380 nm. These peaks are attributed to the transverse modes of a 1-D material with pentagonal cross sections, corresponding to out-of-plane quadrupole and dipole resonance modes. In the present work, as shown in Figure 3-(IV), the SPR absorption band clearly shows two characteristic peaks at 351 and 365 nm, indicative of wires of small-diameter. It is important to note that these two SPR peaks appear at significantly shorter wavelengths than noted above or wires with diameters between 30 and 60 nm.[27, 28] As well as causing a blue-shift

in the peaks, a reduction in the NWs diameter, also reduces the amount of scattered light. It is known that the extinction coefficient depends on both the damping constant and dielectric function.[30] For smaller sized Ag NWs, the variation in scattering intensity along the nanowires and the polarization of the nanowires by the electromagnetic field can change the damping constant and dielectric function as well as the shape of the SPR bands.[31]

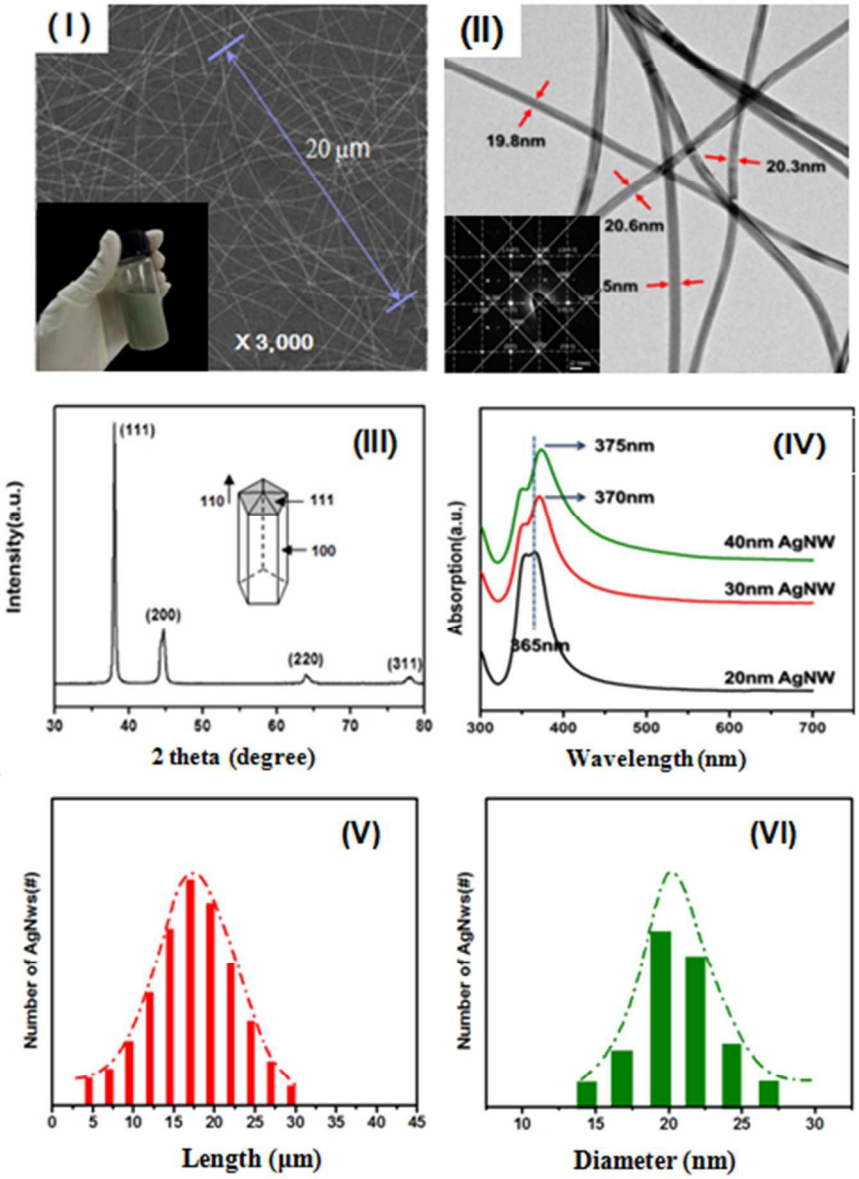

Figure 3

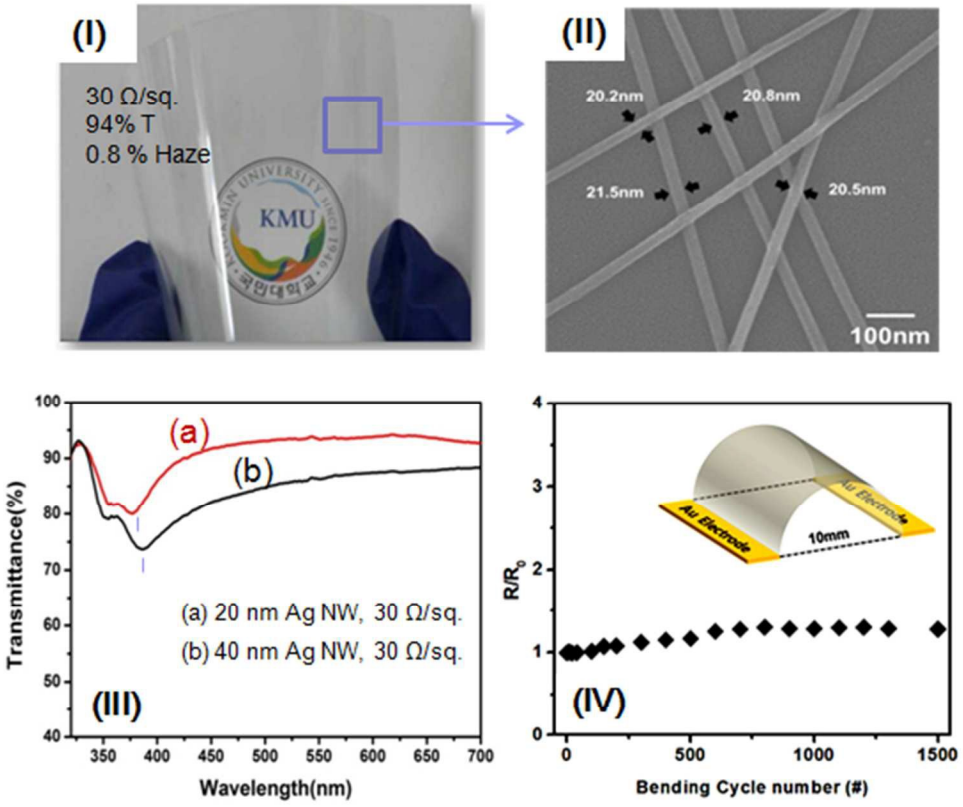

Figure 4

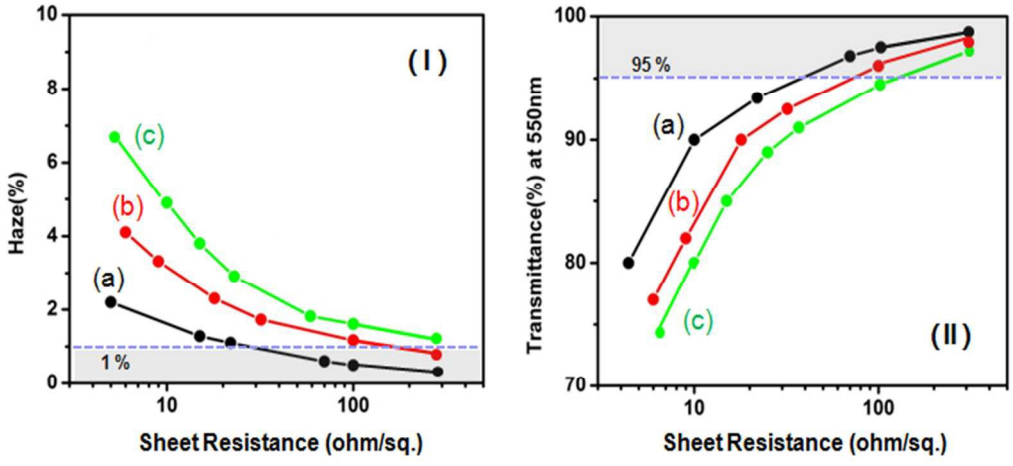

Figure 5

The Ag NWs, with diameters of approximately 20-nm and lengths of 20-μm, were dispersed in DI water at an optimized density of 0.5 mg/mL and deposited on a plasma-treated PET substrate film using a commercially available wet coating method (e.g., spin coating and Mayer bar coating) for fabrication of a transparent electrode film. The highly conductive Ag NWs electrode films are obtained without any post-treatment. In Figure 4, these 2-D cast films, consisting of networks of Ag NWs, show a sheet resistance of 30 Ω/sq., a transmittance of 94% and a low haze value of 1.0% at 550 nm wavelength. This sheet resistance almost matches the electrical properties of ITO films (i.e., a sheet resistance of ≤ 30 Ω/sq with transmittance of 95% and haze value of ≤1.0). The light transmittance spectrum of as-cast 20-nm diameter Ag NW networked films, with 40-nm diameter Ag NW films for comparison, was measured using UV-Vis spectrometry and is shown in Figure 4-(III). The film sample with 20-nm diameter Ag NWs showed excellent light transmittance of 94 % and a haze value of 1.0% at 550 nm wavelength (PET film based), with a sheet resistance of 30 Ω/sq. On the other hand, that of 40-nm diameter Ag NW sample showed a light transmittance of 88 %, and haze value of 2.5%, for the same sheet resistance. This difference of 6% in transmittance is likely associated with the higher value of haze, which results from light scattering. Haze factor is a standard metric for quantifying a film's light scattering efficiency. It is thus a critical parameter for optoelectronic devices, and is defined according to Eq. (b); T_{diff} is the percentage of light diffusively scattered and T_{tot} is the total light transmitted.

(b) $Haze\ (\%) = T_{diff} / T_{tot} \times 100$

Haze values appear to be strongly dependant on network density or size. Figure 5 shows, the haze and light transmittance of as-cast Ag NW networked films with NW diameters of 20-nm, 30-nm, and 40-nm as function of sheet resistance in the range 5−300 Ω/sq. As shown in curve (a) of Figures 5-(I) and (II), the Ag NW film with 20-nm diameters showed a low haze value of ≤1.0, with optical transmittance value up to 95 %, for samples with a sheet resistance of more than 30 Ω/sq. This optical properties data is superior to that of the 30-nm and 40-nm diameter samples, shown in curve (b) and (c) of Figure 5. In particular, for the same sheet resistance, the light transmittance of the Ag NW film of 20-nm diameter was at least 3˜5% more than that of Ag NW film of 40-nm diameter. The haze value, in the case of wires of 20 nm diameter, was at least 1˜2% less than the 40 nm diameter wires, as shown in Figure 5-(I). Such a large reduction in transmittance or haze is attributed to the effects of NW diameter. Overall, it is seen that the optical properties of Ag NW network films with small diameter NWs were superior to those with larger diameters and, in particular, the level of haze is largely influenced by the ability of Ag NWs to scatter light. As a result, 2-D Ag films formed by a network of 20-nm sized NWs could produce a sufficiently transparent electrode film for electronic devices, owing to the low intensity of scattered light. By current standards, transparent electrode films, with high transmittance and a haze value of at most 1.5% are considered very useful for electronic devices. However, the 2-D Ag NW films formed by a network of 20-nm diameter NWs have optical properties sufficiently comparable to ITO. Additionally, Ag NWs network films with small diameter NWs are expected to show better flexibility; bending test is shown in Figure 4-(IV). To test for mechanical flexible stability of the Ag NW films, a bending test system was designed as shown in Fig. 4-(IV). The system consisted of the two contact lines: one of the lines was fixed and the other could be moved laterally. In this test, the bending is rolled at a distance with

diameter of 10 mm, subsequently unrolled at speed of 20 mm s^{-1}, and the sheet resistance of film is compared to its initial value. Fig. 4-(IV) show a result of the changes in the resistances of the electrode film using the Ag NWs (sheet resistance, 30 Ω/sq) as a function of bending cycle number. The percentage change in the resistance of the flexible Ag NWs film can be expressed as 0.5% or less after being 1500 times, verifying that the 20-nm-diameter Ag NWs film possesses an excellent mechanical flexibility, although no significant difference between them of 40-nm-diameter.

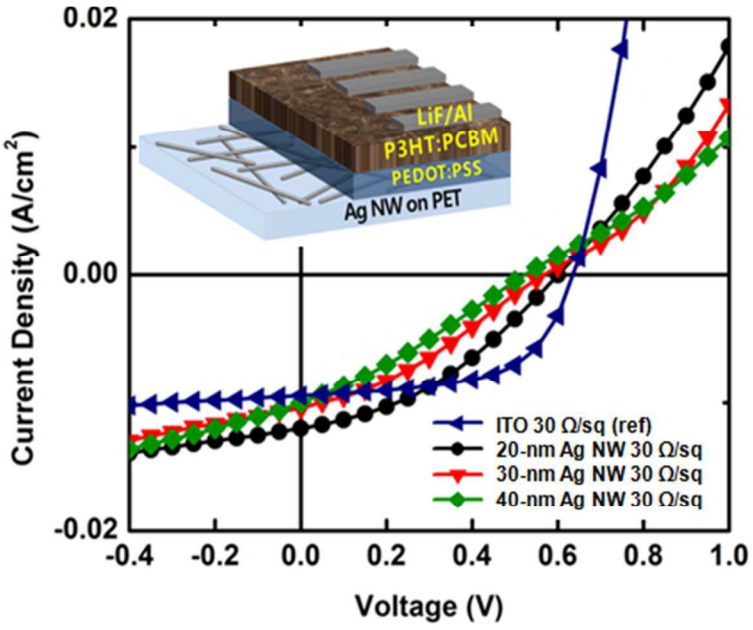

	Voc (V)	Jsc (mA/cm²)	FF	PCE (%)
ITO(Ref.)	0.61	10.40	0.46	2.93
20 nm AgNW	0.60	11.98	0.37	2.69
30 nm AgNW	0.57	10.41	0.33	1.93
40 nm AgNW	0.52	9.99	0.29	1.51

Figure 6

The following are necessary criteria for transparent electrodes with a plastic substrate, in order to

be used in organic photovoltaic (OPV) devices or organic light-emitting diodes (OLED): a sheet resistance of about 10–30 Ω/sq, light transmittance higher than 90%, and a low haze value, at most 1.5%. Many research groups are beginning to incorporate Ag NW films fabricated by printing method as front electrodes for solar applications.[32-34] Depending on the experimental conditions used for their application, Ag NW films could have haze factors varying between 2 and 10%. If low haze value is desired for devices, it could be achieved by size controls of Ag NWs such as increasing length and decreasing diameter which can lead to haze value below 1.5%.[20, 21] Moreover, smaller diameter Ag NWs can directly decreases the haze in the visible range because of the decreasing scattering of light. Additionally, to achieve sufficiently transparent electrode films having a high transparency of more than 90 % (level of ITO) with 30 ohm/sq sheet resistance for solar applications, the transparent electrode films of low haze value are need. If the transmittance and haze value at the same conductive range can be as ITO level, Ag NW electrodes will open new capability for solar applications. In order to investigate the performance for practical application of the electrode films formed by a network of 20-nm diameter NWs in flexible OPVs, cells were fabricated based upon the following architecture: 125 μm PET film/Ag NWs/PEDOT:PSS/P3HT:$PC_{60}BM$/LiF/Al. Figure 6 shows current density-voltage (*J-V*) characteristics of flexible OPVs with Ag NW transparent electrodes, as well as a rigid ITO electrode device for reference, measured under AM 1.5 G illumination and in the dark. The reference device with an ITO electrode on glass (with a sheet resistance of 30 Ω/sq) exhibited the power conversion efficiency (PCE) of 2.93 % and a fill factor (FF) of 0.46. In comparison, the cell using 20 nm diameters Ag NW-networked film on PET exhibited a PCE of 2.69% and a FF of 0.37, sufficiently comparable to the reference ITO on electrode. On the other hand, the OPV cells with 30 nm and 40 nm diameters Ag NW-networked film electrodes (sheet

resistance of 30 Ω/sq, optical transmittance of 90-92 % and a haze value of 1.7-2.5%), showed lower PCEs of 1.93 and 1.51%, respectively. However, the OPV cell using 20 nm diameters Ag NW-networked electrode on PET film exhibited a PCE of 2.69% almost similar to the ITO on glass. The relatively higher PCE of the 20 nm diameter Ag NW film is considered to have been caused to more intense absorption in the active layer from a higher optical transmittance resulting from low haze value. As shown in curve (a) of Figures 5, the Ag NW film with 20-nm diameters showed a relatively lower haze value than those of 30-nm and 40-nm diameter samples. On the other hand, the light transmittance of the Ag NW film of 20-nm diameter showed at least 3~5% higher than those of Ag NW film of 30-nm and 40-nm diameter.

CONCLUSION

The present work demonstrates that thin Ag NWs with diameter in the range of 16−22 nm can be synthesized using a high-pressure polyol method. Ag NWs of pentagonal-structure twinned along the [111] plane are subsequently produced, and the nanowire dimensions, particularly the diameter, can be controlled by the process pressure. Additionally, the characteristic SPR of thin Ag NWs was observed at 365 nm in the absorbance spectrum, which is evidence for the formation of NWs. Furthermore, the 2-D percolating Ag network was found to have a sheet resistance of 30 Ω/sq and an optical transmittance of 94%. The high transmittance is the result of reduced light scattering, which yields a low haze value of ≤1.0%, and with a sheet resistance of 30 Ω/sq, is suitable for electronic display applications. In particular, the OPV cell using 20 nm diameters Ag NW-networked electrode film exhibited a PCE of 2.69% with a FF of 0.37, sufficiently comparable to the reference ITO on electrode. However, even for the 20-nm Ag NW cell, the PCE of OPV devices is consistently 0.24 lower than that of corresponding ITO glass-

based devices, significantly reducing their observed efficiency. On the other hand, this study demonstrates that the 20 nm-diameter Ag NW electrode satisfies the important criteria of conductivity, transparency, haze, and solution-processability necessary to replace ITO in electronic displays. It is obvious that these transparent conducting Ag NW films have the potential to outperform conventional ITO, especially when considered as a possible electrode layer in flexible devices.

ACKNOWLEDGMENTS

This work was financially supported in part by the Converging Research Center Program through the Ministry of Science (ICT and Future Planning) (2013K000201), and the Industrial Core Technology Development Project through the Ministry of Knowledge and Commerce (10035644 and 10035648).

Corresponding Author

**Jin-Yeol Kim*

School of Advanced Materials Engineering, Kookmin University, Seoul 136-702, Korea

Electronic mail : jinyeol@kookmin.ac.kr, Tel: +82-2-910-4663

FIGURE CAPTIONS

Figure 1 Two-step reaction scheme for synthesizing Ag NWs through a high-pressure polyol process. (a) under 0 psi pressure, 30-nm sized Ag seed crystals with multi-twin structure are

formed through reduction of $AgNO_3$, and grown to wires with diameters of about 30-nm. (b) under 1000 psi (69 bar) pressure, 20-nm sized Ag particles are formed and grown to 20-nm wires.

Figure 2 (a) Diameter of Ag NWs grown, as a function of pressure in the range 0-1000 psi (69 bar). In the absence of KBr, the diameter of Ag NWs is not influenced by pressure regardless of $NaCl/AgNO_3$ concentration. However, for a molar concentration ratio of NaCl/KBr = 2, the diameter of Ag NWs is decreases with increased pressure.
(b) Diameter of Ag NWs as a function of KBr concentration, for pressures 0 and1000 psi (69 bar). Upper data set is measured at low NaCl concentration (mole concentration ratio of $NaCl/AgNO_3$ =0.0065) and lower is at high NaCl concentration ($NaCl/AgNO_3$ =0.167). The diameters of the synthesized Ag NWs were determined from the mean value of wires per each sample, and the mean value was counted from more than 100 wires. Samples of each specimen were also confirmed from the 5 batch or more synthesis.

Figure 3 (I) SEM and (II) TEM image of Ag NWs with lengths of 20-μm and 20-nm diameters, synthesized using a high-pressure polyol reaction. The inset of (II) displays the SAED pattern of the Ag NW with a twinned structure. (III) XRD pattern and (IV) SPR absorption characteristic of the synthesized Ag NWs with 20-nm, 30-nm, and 40-nm diameters. Distributions of the length (V) and the diameter (VI) of synthesized Ag NWs.

Figure 4 (I) Optical image of the transparent electrode film containing Ag NWs of 20-μm lengths and 20-nm diameters, and (II) SEM morphologies of the resulting randomly dispersed Ag NW network film. (III) Light transmittance spectra of the transparent electrode Ag NW film (PET-based) with 30 ohm/sq sheet resistance; (a) 94% transmittance for the sample containing Ag NWs 20 nm in diameter and (b) 86% transmittance for Ag NWs 40 nm in diameter. (IV) Change of sheet resistance after a bending test of 1500 cycles.

Figure 5 Changes of (I) haze value and (II) optical transmittance measured at various sheet resistance conditions for Ag NW transparent electrode films. Legend: (a) films containing Ag NWs of 20-nm, (b) 30-nm, and (c) 40-nm diameter (the average length of the wire samples are

18~20-μm, 20~24-μm, and 20~25-μm, respectively). Haze value and transmittance were measured at 550 nm wavelength.

Figure 6 Device structure and current density–voltage characteristics of OPVs using a Ag NW layer with 20-nm, 30-nm, and 40-nm diameter (the average length of the wire samples are 18~20-μm, 20~24-μm, and 20~25-μm, respectively), NWs as the transparent electrode (reference curve; solar cell with an ITO electrode on glass). The table is a summary of the performance parameters of OPVs based on ITO/glass and Ag NW/PET.

Reference

1. S. Ye, A. R. Rathmell, Z. Chen, I. E. Stewart and B. J. Wiley, *Adv. Matter.* 2014, **26**, 6670.
2. Y. Wu, J. Xiang, C. Yang, W. Lu and C. M. Lieber, *Nature*, 2006, **430,** 61.
3. A. Strevens, A. Drury, S. Lipson, M. Kröll, W. Blau and H. Hörhold, *Appl. Phys. Lett.*, 2005, **86,** 143503.
4. E. Zimmermann, P. Ehrenreich, T. Pfadler, J. A. Dorman, J. Weickert and L. Schmidt-Mende, *Nature Photonic,* 2014, **8,** 669.
5. C. Preston, Y. Xu, X. Han, J. N. Munday and L. Hu, *Nano Research*, 2013, **6**, 461.
6. A. Aleshin, S. Williams and A. S. Heeger, *Synth. Met*., 1998, **94**, 173.
7. T. Granlund, L. A. Pettersson and O. Inganäs, *J. Appl. Phys*., 2001, **89**, 5897.
8. J. Hu, T. W. Odom and C. M. Lieber, *Accounts of Chemical Research,* 1999, **32**, 435.
9. Z. W. Pan, Z. R. Dai and Z. L. Wang, *Science*, 2001, **291**, 1947.
10. M. A. El-Sayed, *Accounts of chemical research,* 2001, **34**, 257.
11. J. Y. Lee, S. T. Connor, Y. Cui and P. Peumans, *Nano Letters,* 2008, **8**, 689.
12. H.-Y. Lu, C.-Y. Chou, J.-H. Wu, J.-J. Lin and G.-S.Liou, ***J. Mater. Chem. C***, 2015, **3**, 3629.
13. J. Liang, L. Lu, K. Tong, Z. Ren, W. Hu, X. Niu, Y. Chen and Q. Oei, ACS Nano, 2014, **8**, 1590.
14. Y. Sun, B. Sun, B. Mayers and Y. Xia, *Nano Lett.* 2002, **2**, 165.
15. Y. Sun,Y. Yin, B. T. Mayers, T. Herricks and Y. Xia, *Chemistry of Materials*, 2002, **14**, 4736.
16. Y. Xia, P. Yang, Y. Sun, Y. Wu, B. Mayers, B. Gates, Y. Yin, F. Kim and H. Yan, *Adv. Mater*. 2003, **15**, 353.
17. B. Wiley, Y. Sun, J. Chen, H. Cang, Z-Y. Li, X. Li and Y. Xia, *MRS Bull.*, 2005, **30**, 356.

18. T. Kim, A. Canlier, G. H. Kim, J. Choi, M. Park and S. M. Han, *ACS Appl. Mater*. *Interfaces*, 2013, **5**, 788.

19. T. Araki, J. Jiu, M. Nogi, H. Koga, S. Nagao, T. Sugahara and K. Suganuma, *Nano Research*, 2014, **7**, 236.

20. M. H. Chang, H. A. Cho, Y. S. Kim, E. J. Lee and J. Y. Kim, *Nanoscale Res Lett.*, 2014, **9**, 330.

21. C. Preston, X. Han, J. N. Munday and L. Hu, *Nano Res.*, 2013, **6**, 461.

22. E. J. Lee, M. H. Chang, Y. S. Kim and J. Y. Kim, *APL. Mater.*, 2013, **1**, 042118.

23. F. Fievet, J. Lagier and M. Figlarz, *MRS Bulletin*, 1989, **14**, 29.

24. X. Tang, M.Tsuji, M. Nishio and P. Jiang, *Bull. Chem. Soc. Jpn.*, 2009, **82**, 1304.

25. S. C.Liao, W. E. Mayo and K. D. Pae, *Acta Mater.,* 1997, **45**, 4027.

26. J. P. Kottmann, O. J. F. Martin, D. R. Smith and S. Schultz, *Physical Review B*, 2001, **64**, 235402.

27. Y. Sun, Y. Xia, *Analyst*, 2003, **128**, 686.

28. J. Mock, M. Barbic, D. Smith, D. Schultz and S. Schultz, *The Journal of Chemical Physics*, 2002, **116**, 6755.

29. B. J. Wiley, S. H. Im, Z-Y. Li, J. McLellan, A. Siekkinen and Y. Xia, *The Journal of Physical Chemistry B*, 2006, **110**, 15666.

30. P. N. Prasad, 2004 *Nanophotonics*, John Wiley & Sons.

31. J. Mock, S. Oldenburg, D. Smith, D. Schultz and S. Schultz, *Nano Lett.,* 2002, **2**, 465.

32. L. Yang, T. Zhang, H. Zhou, S. C. Price, B. J. Wily and W. You, *ACS Appl. Mater. Interfaces*, 2011, **3**, 4075.

33. W. Gaynor, J. Y. Lee and P. Peumans, *ACS Nano*, 2010, **4**, 30.

34. C. C. Chen, L. Dou, R. Zhu, C-H. Chang, T-B. Song, Y. B. Zheng, S. Hawks, G. Li, P. S. Weiss and Y. Yang, *ACS Nano*, 2012, **6**, 7185.